

Liang A et al. (2021) AUCUBIN ENHANCES LPS-INDUCED PROLIFERATION AND APOPTOSIS MITIGATION VIA UPREGULATING MICRORNA-9 IN CARTILAGE CELLS: IMPLICATIONS FOR MENTAL AND PHYSICAL HEALTH. Revista Internacional de Medicina y Ciencias de la Actividad Física y el Deporte vol. 21 (82) pp. 419-431

DOI: <https://doi.org/10.15366/rimcafd2021.82.014>

ORIGINAL

AUCUBIN ENHANCES LPS-INDUCED PROLIFERATION AND APOPTOSIS MITIGATION VIA UPREGULATING MICRORNA-9 IN CARTILAGE CELLS: IMPLICATIONS FOR MENTAL AND PHYSICAL HEALTH

Shi Feng^{1#}, Di Fu^{2#}, Liang A^{1*}

¹Department of Second Orthopedics, Affiliated Central Hospital of Shenyang Medical College, Shenyang, 110000, China

²Department of General Medicine, Affiliated Central Hospital of Shenyang Medical College, Shenyang, 110000, China.

#These authors contributed equally: Shi Feng and Di Fu

E-mail: llianganb@163.com

Recibido 6 de junio de 2019 **Received** June 6, 2019

Aceptado 24 de noviembre de 2019 **Accepted** November 24, 2019

ABSTRACT

This research delves into the effects of Aucubin (Au) on LPS-induced inflammation in cartilage cells, with an emphasis on its implications for mental and physical health in osteoarthritis (OA). We analyzed the impact of Au on cell viability, apoptosis, and inflammatory markers, and further explored its regulatory influence on microRNA-9 (miR-9). Our results show that Au effectively mitigates LPS-induced damage in cartilage cells by modulating miR-9, subsequently influencing the NF- κ B pathway. This study sheds light on the potential of Au in enhancing both mental and physical health aspects in OA, proposing a novel therapeutic avenue for comprehensive OA management.

KEYWORDS: Aucubin (Au); Osteoarthritis (OA); miR - 9; Physical health

1. INTRODUCTION

The research begins by explaining the role of Lipopolysaccharides (LPS), a component of the outer membrane of certain bacteria, in inducing cellular stress and apoptosis (programmed cell death) in cartilage cells. This process is particularly relevant in the context of joint diseases such as osteoarthritis, where inflammation and cartilage degradation are key issues (Cao, Li, Tang, Ding, & Hunter, 2020). Aucubin, a compound traditionally recognized for its therapeutic properties in herbal medicine, is then introduced as a potential modulator of

these processes (Cui et al., 2020; Lewis et al., 2019). The study delves into the molecular mechanisms of aucubin's action, particularly highlighting its role in upregulating MicroRNA-9. MicroRNA-9 is a small non-coding RNA molecule that plays a crucial role in regulating gene expression, and its upregulation by aucubin appears to counteract the negative effects of LPS on cartilage cells (An et al., 2020; Chen et al., 2017).

The pivotal point of the study is the demonstration that aucubin not only enhances cell proliferation in cartilage cells exposed to LPS but also mitigates apoptosis. This dual action suggests a protective and restorative effect of aucubin on cartilage cells, which could have significant implications for the treatment of joint diseases (Madzuki, Lau, Che Ahmad Tantowi, Mohd Ishak, & Mohamed, 2018; Madzuki, Lau, Mohamad Shalan, Mohd Ishak, & Mohamed, 2019).

Beyond the direct implications for joint health, the study also explores the broader impacts on mental and physical health. Chronic joint diseases often lead to reduced mobility and chronic pain, which can have profound effects on mental health, including increased risk of depression and anxiety. By potentially offering a novel approach to treating joint disease, this research suggests a pathway not only to improved physical health but also to better mental well-being (Conaghan, Cook, Hamilton, & Tak, 2019; Griffin & Scanzello, 2019; Woodell - May & Sommerfeld, 2020).

Aucubin, (Au, β -D-glucopyranoside), as shown in Figure 1, one of the extracts of *Eucommia ulmoides*, *Plantago depressa* Willd, and *Rehmannia glutinosa*, has the functions of clearing dampness and heat, promoting urination, analgesia, reducing blood pressure, protecting liver and anti-tumor, promote the regeneration of stem cells and significantly inhibit the replication of hepatitis B virus DNA (Liu et al., 2021; Xue, Chen, Zhang, & Li, 2019).

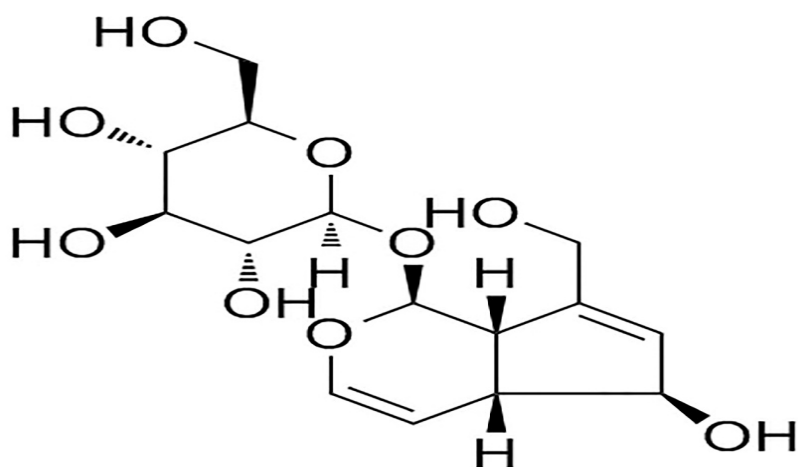


Figure 1: Structural formula of Au

The study's comprehensive approach, combining molecular biology with

a focus on holistic health outcomes, makes it a significant contribution to the field. It paves the way for future research into the use of natural compounds like aucubin in medical treatments and highlights the importance of understanding the complex interplay between physical and mental health (Jian, Su, Zhou, & Xiong, 2020; PARENTI, 2019; Zhang et al., 2021).

2. Materials and Methods

2.1 Cell culture and treatments

The cartilage cells (Wuhan punuosai Life Technology Co., Ltd, Wuhan, China) were cultured with DEME (Gibco, New York, USA), including 10% fetal bovine serum (Gibco), were fostered in a wet incubator filled with 5% CO₂ and 95% air at 37°C. The culture medium was renewed every 3 days. Then, the cells were incubated in DEME including change doses of LPS (2.5, 5, 7.5, and 10 µg/ml) under 37°C for 12h. Au was dissolved with the final concentration at 10, 100, 200, 400, and 800 µM. For Au administration, the cells were cultured in DEME containing Au (10, 100, 200, 400, 800 µM) for 36 h before LPS stimulation.

2.2 Cell viability experiment

After stimulation with LPS or Au, cell viability was tested using a Cell Counting Kit-8 (CCK-8; Fuzhou Feijing Biotechnology Co., Ltd, Fujian, China). The cells were cultured in a 96-well plate at some 5×10^3 cells/well and overnight under 37°C. Then, 10 µl of CCK-8 working medium was added and the cells were cultured for 1 h under 37°C. The absorbance values were measured using a microplate reader (Bio-Rad, Hercules, CA, USA) with 450 nm.

2.3 Apoptosis experiment

Apoptosis was tested using an Annexin V-FITC/PI Apoptosis Detection Kit (Beyotime Biotechnology, Shanghai, China). Briefly, Step 1: the cells were cultured at some 1×10^5 cells/well in 6-well plates. Step 2: the cells were collected and washed with PBS. Step 3: the cells were suspended in binding buffer and were cultured by the presence of Annexin V-FITC and PI in a dim place. Step 4: Stained cells were set to a flow cytometer (Beckman Coulter, Fullerton, CA, USA) to separate apoptotic or necrotic cells. The percentage of apoptosis was calculated using the FlowJo software (Tree Star, San Carlos, CA).

2.4 ELISA

After the operation, the concentration of pro-phlogistic factors, including IL-6, TNF- α , and IL-1 β was tested by an Elisa kit (Ray Biotech, Atlanta, USA).

Briefly, the standard and samples to be checked were put to the corresponding wells, followed by incubation with the detector antibody labeled with horseradish peroxidase. The plate was covered with sealing film and incubated under a 37 °C water bath for 1 h.

The reaction liquid was discarded, and the plate dried with filter paper after washing, then incubation with the corresponding substrate under 37 °C in a dim place for 15 min. Finally, 50 µL working fluid was put in, and within 15 min, OD values at a wavelength of 450 nm were tested via a microplate reader (Bio-Rad, Hercules, CA, USA).

2.5 microRNA (mir) transfection

miR-9 mimic, miR-9 inhibitor, and Phage NC (NC) were compounded via Ribobio, (Guangzhou, China). miRs (50 nM) were separately transfected into cells through riboFECT™ CP (Ribobio) following the producer's protocol.

2.6 RT-qPCR

After the treatments, all RNA was obtained through TRIzol reagent (Ray Biotech). According to the respective manuscript instructions, total cDNA and miR-specific cDNA were synthesized through the SuperScript® VILO™ cDNA Synthesis Kit (Ray Biotech) and TaqMan™ MicroRNA Reverse Transcription Kit (Thermo Fischer, Shanghai, China), respectively. For real-time PCR, Power SYBR™ Green PCR Master Mix (Thermo Fisher) was applied for the quantification of miR-9 and mRNAs, as suggested by the manufacturer. The results were computed following the $2^{-\Delta\Delta Ct}$ method. The sequences of the required primers are shown in Table 1.

Table 1 The sequences of the required primers

NAME	FORWARD PRIMER (5' -3')	REVERSE PRIMER (5' -3')
IL-6	TAGTCCTTCCCTACCCCAATTTCC	TTGGTCCTTAGCCACTCCTTC
TNF--α	CACGCTCTTCTGTCTACTGAAC	ATCTGAGTGTGAGGGTCTGG
IL-1β	TGCCACCTTTTGACAGTGATG	GGTCCACGGGAAAGACAC
β-actin	AATGTGTCCGTCGTGGATCT	GGTCCTCAGTGTAGCCCAAG
miR-9	GGACGGACAGCGAGAGGAGGCC AAA	TTTGGCCTCCTCTCGCTGTC CGTCC
U6	CTCGCTTCGGCAGCACA	AACGCTTCACGAATTTGCGT
miR-9 mimic	UCUUUGGUUAUCUAGCUGUAUG A	AUACAGCUAGUAACCAAAG AUU
miR-9 inhibitor	UCAUACAGCUAGUAACCAAAGA	
NC	UCACAACCUCCUAGAAAGAGUAG A	UCACAACCUCCUAGAAAGAG UAGA

2.7 Western blot

The cells were collected and dissociated in RIPA lysis buffer (Beyotime Biotechnology). Whole-cell lysates were centrifuged at 4°C (12000×g, 15 min), and the proteins in the supernatant were quantified using a BCA™ Protein Assay Kit (Biotechnology).

Proteins (25 µg/hole) were separated through 12% SDS-PAGE, and the proteins in the gels were blotted to PVDF membranes (Shanghai Epizyme Biomedical Technology Co., Ltd, Shanghai, China). After blocking in 5% nonfat milk, PVDF membranes were incubated with a primary antibody and an HRP-conjugated secondary antibody (Abcam, Cambridge, MA, USA) in the proper order.

The primary antibodies used in this paper included antibodies pro-caspase-3, cleaved caspase-3, Bcl-2, Bax, IκBα, p-IκBα, p65, p-p65, or β-actin (all Abcam). Proteins in the PVDF membranes were observed via an ECL detection system (Bio-Rad, Hercules, CA, USA). The value of bands was calculated using the ImageJ software (National Institutes of Health, Bethesda, MA).

2.8 Statistical analysis

Experimental data was duplicated three times. The data were shown as mean ±SD. Statistical analysis was handled using the Graphpad Prism 7 software (GraphPad, San Diego, CA). The *P* values were computed via the ANOVA method. *P* < 0.05 indicated statistically significant data.

3 Results

3.1 LPS induced apoptosis and release of pro-phlogistic factors in the cartilage cells

LPS was used to induce inflammatory injury in cartilage cells. Under stimulation with LPS, the cell viability was prominently declined through LPS at the concentration of 2 (*P* < 0.05), 4, 6, 8, and 10 µg/mL (*P* < 0.001), as compared with the natural cells, as shown in Figure 2A.

Meanwhile, the percentage of apoptosis in the 4 µg/mL LPS was risen than that in the 0 µg/ml LPS group (*P* < 0.05), as shown in Figure 2B. As shown in Figure 2C and Figure 2D, stimulation with 4 µg/mL LPS induced a remarkable raise in cleaved caspase-3 and Bax, while a marked reduction of Bcl-2 (*P* < 0.05). Hence, 4 µg/ml was selected as the working concentration in the after tests.

As shown in Figure 2E and Figure 2F, the expression of pro-phlogistic factors was also memorably heightened after LPS stimulation (*P* < 0.001). The

results hinted that inflammatory injury of cartilage cells was well induced.

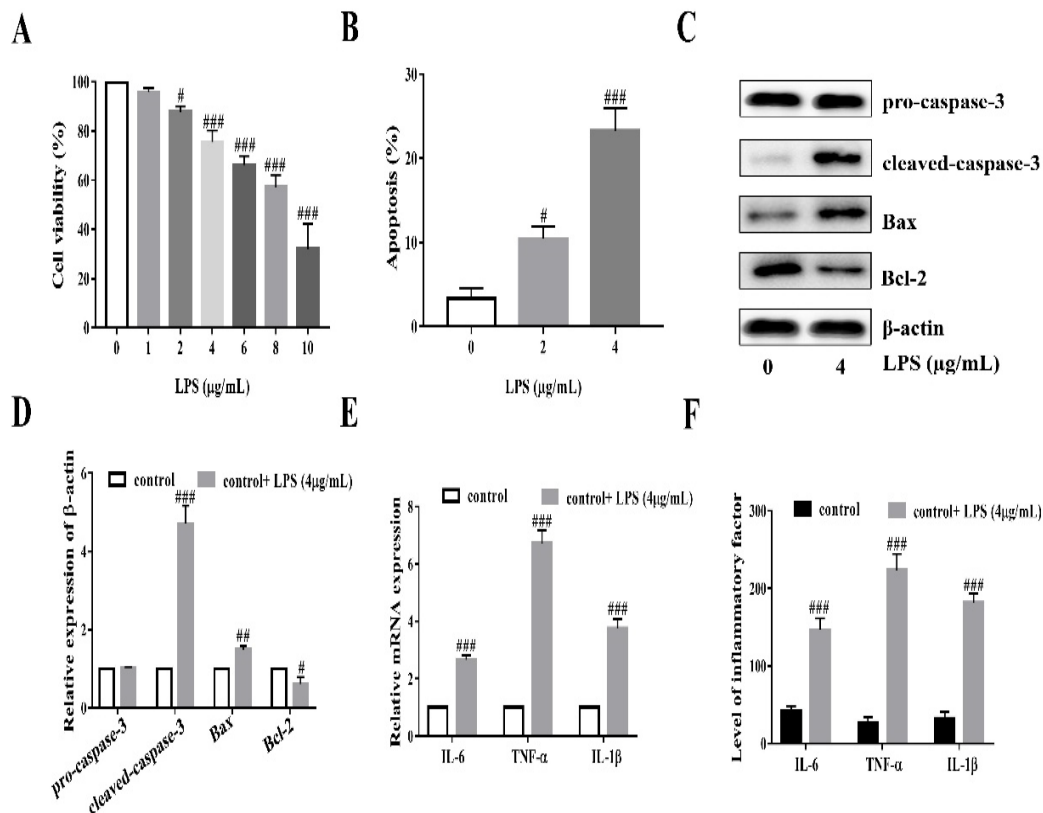


Figure 2: Selection of LPS, detection of apoptosis related proteins and inflammatory factors
A: Gradient setting of LPS. B: Effect of LPS (0, 2, 4µg/mL) on apoptosis. C: Protein band. D: Protein statistical chart. E: The expression of inflammatory factors was detected using the RT-PCR; F: The level of inflammatory factors was detected using ELISA. #P< 0.05, ##P<0.01, ###P<0.001 control VS LPS.

3.2 Au reduced LPS-induced changes in the cartilage cells

To appraise the toxic consequence of Au, the cells were administered by rising concentrations of Au (0–800 µM), followed by measurements of the cell viability. As shown in Figure 3A, 25, 50, 100, 200, 400 µM Au showed non-statistical significance for cell viability.

We used 400µM in the latter test. Next, we searched the effects of Au safeguards on LPS-stimulated inflammatory cellular injury. Interestingly, LPS-induced abatement of cell activity (Figure 3B), promotion of apoptosis (Figure 3C), diversification of relative proteins (Figure 3D, E).

And discharge of proinflammatory cytokines (Figure 3F, G) were all dramatically weakened by Au administration corresponding to the LPS group ($P < 0.05$). Therefore, the data collectively make known that Au could mitigate LPS-caused inflammatory cell damage in cartilage cells.

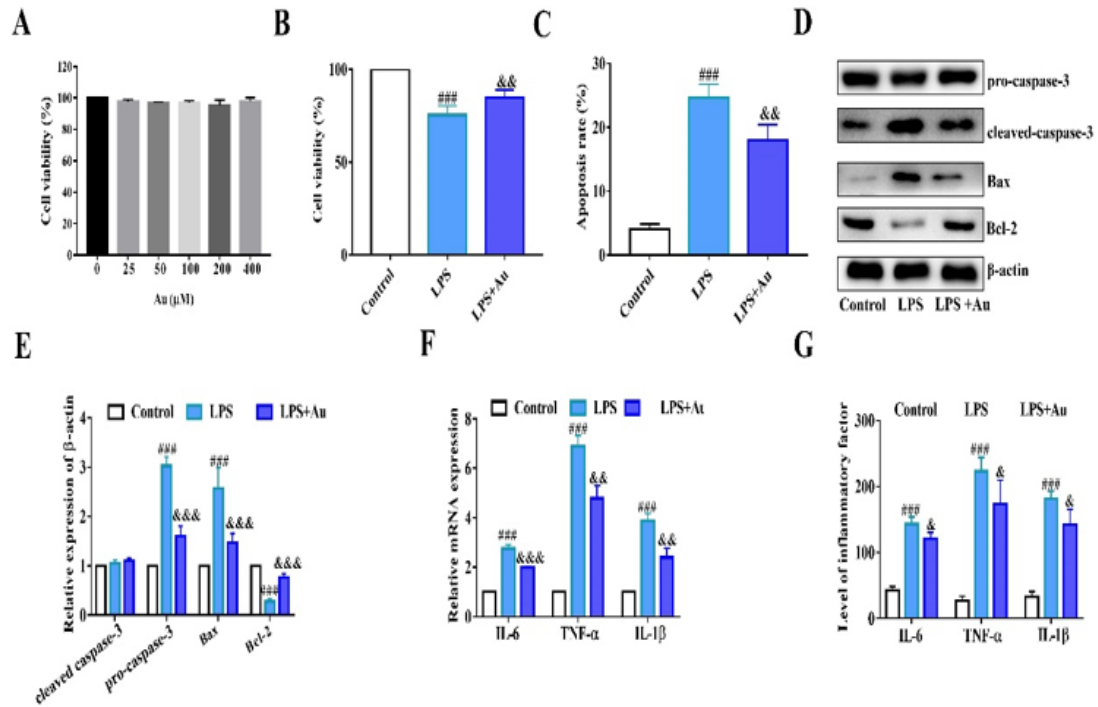


Figure 3: Drug concentration selection and index detection, A: Toxicity test of Au; B: Effect of Au on LPS induced cell viability recovery; C: Effect of Au on LPS induced apoptosis recovery; D, E: Protein bands and statistical chart; F: The expression of inflammatory factors was detected using the RT-PCR; G: The level of inflammatory factors was detected using ELISA. ### $P < 0.001$, control VS LPS, & $P < 0.05$, && $P < 0.01$, &&& $P < 0.001$, LPS VS LPS + Au.

3.3 Au regulated miR-9 in cartilage cells

The level of endogenous miR-9 after LPS or Au administration with LPS provoked was tested. As revealed in Figure 4, the level of endogenous miR-9 was observably descended after LPS stimulation corresponding to the control ($P < 0.05$), and it was further augmented by Au pretreatments corresponding to the LPS group ($P < 0.05$). The results suggested that Au upregulated the levels of miR-9 in cartilage cells, which states clearly that miR-9 was key to regulating Au in cartilage cells.

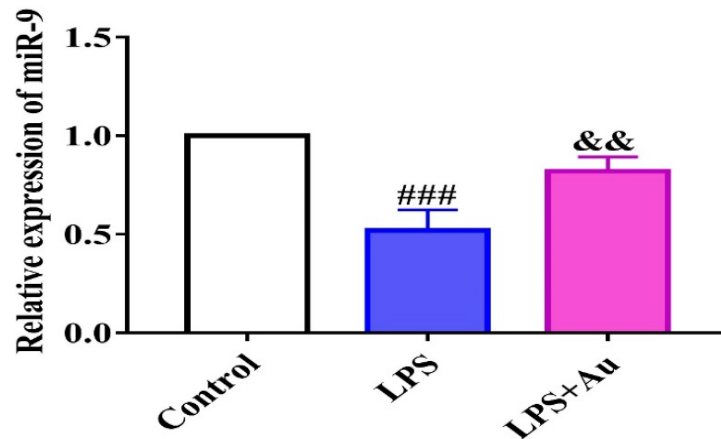


Figure 4 Detection of miR-9 level ### $P < 0.001$, control VS LPS, && $P < 0.001$, LPS VS LPS + Au.

3.4 Au retarded LPS-caused cell injury via regulating miR-9

The latter test was to prove whether Au acts on LPS treated cartilage cells through miR-9. First, cartilage cells with LPS were transfected with miR-9, and Figure 5A showed that the level of miR-9 was prominently enhanced after transfection with miR-9 mimic ($P < 0.05$). Next, the effects of miR-9 on cell vitality (Figure 5B) were increased but apoptosis (Figure 5C), relative proteins (cleaved caspase-3 and Bax) (Figure 5D, and E), emancipation of proinflammatory cytokines (Figure 5F, and G) in LPS-stimulated cartilage cells were memorably weakened after miR-9 upregulation. Nevertheless, the level of miR-9 evidently reduced ($P < 0.05$) after transfection with an miR-9 inhibitor in Au pretreated cells in comparison with NC (Figure 6A). Finally, the effects of Au on cell vitality (Figure 6B) were increased but apoptosis (Figure 6C), relative proteins (cleaved caspase-3, Bax, and Bcl-2) (Figure 6D, E), emancipation of proinflammatory cytokines (Figure 6F, G) in LPS-stimulated cartilage cells were memorably weakened after Au administration, however, these were memorably opposite after miR-9 inhibitor in contrast with NC-transfected cells ($P < 0.05$).

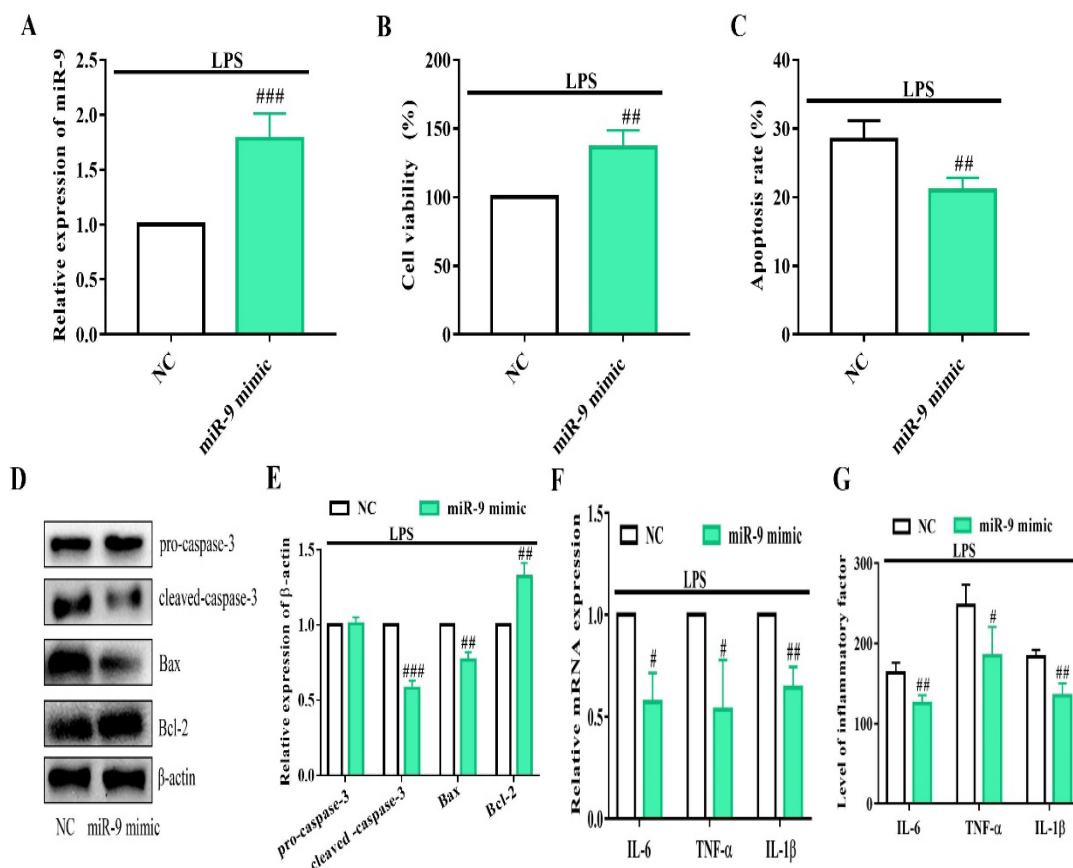


Figure 5 Function detection of miR-9 A: Detection of transfection efficiency; B: Detection of cell viability; C: Effect of miR-9 on apoptosis; D, E: Protein bands and statistical charts; F: The expression of inflammatory factors was detected using the RT-PCR; G: The level of inflammatory factors was detected using ELISA. # $P < 0.05$, ## $P < 0.01$, ### $P < 0.001$. NC VS miR-9 inhibitor.

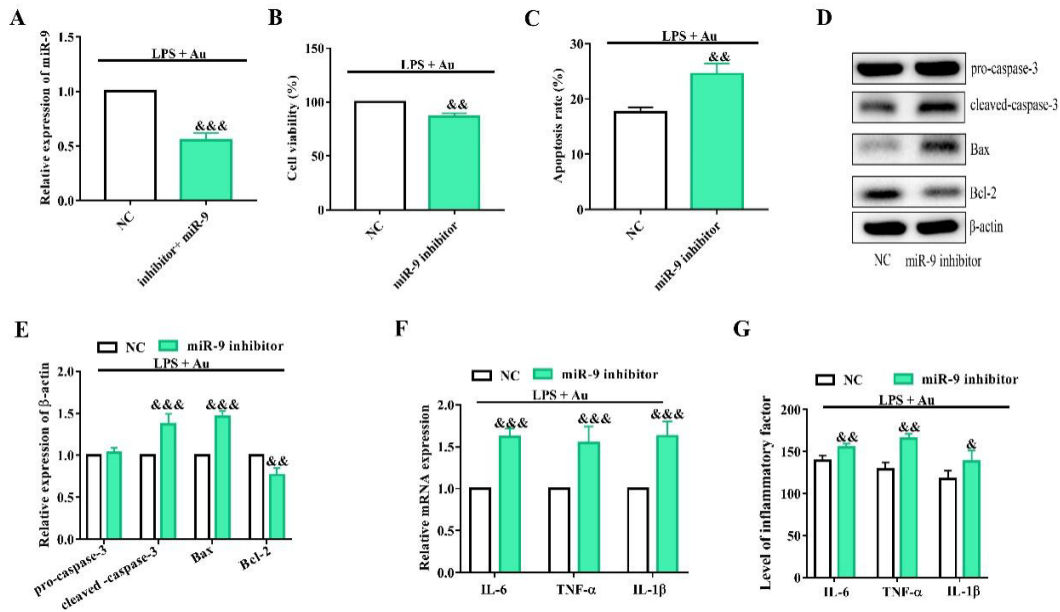


Figure 6: Function detection of miR-9 on Au A: Detection of transfection efficiency; B: Detection of cell viability; C: Effect of miR-9 with Au administration on apoptosis; D, E: Protein bands and statistical charts; F: The expression of inflammatory factors was detected using the RT-PCR; G: The level of inflammatory factors was detected using ELISA. & $P < 0.05$, && $P < 0.01$, &&& $P < 0.001$. NC VS miR-9 mimic.

3.5 Au suppressed the IκBα/NF-κB signaling pathway via regulating miR-9

As shown in Figure 7, Western blot indicated that the phosphorylated standards of IκBα, and p65 were advantageously abated after silencing ($P < 0.05$). In addition, we also observed that the effects of Au on p-IκBα, and p-p65 were sharply raised after miR-9 downregulation ($P < 0.05$). The findings suggested that Au inhibited the NF-κB signaling pathways through regulating miR-9 in LPS-stimulated cartilage cells.

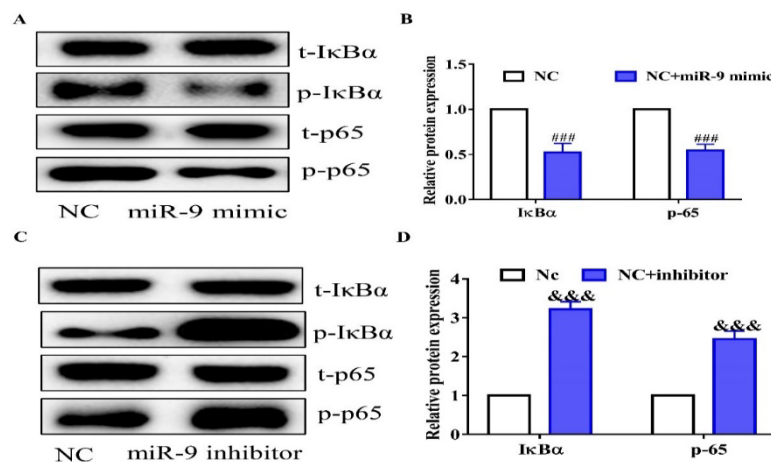


Figure 7: Effect of miR-9 or Au on signal pathway. A, B: Protein bands and statistical charts; C, D: Protein bands and statistical charts. ### $P < 0.001$. NC VS miR-9 mimic, &&& $P < 0.001$. NC VS miR-9 inhibitor.

4. Discussion

At present, the treatment strategies of OA, such as visco supplement, pain control and joint replacement, are only for the late symptoms of OA. However, the therapeutic results are still far from satisfactory. This study established an inflammatory model through cartilage cells and confirmed that Au pretreatments could relieve inflammatory hurt in vitro. Then, we found that LPS induced downregulation of miR-9 was prominently upregulated by Au pretreatments. In addition, the effects of Au on LPS-stimulated cartilage cells were enhanced after miR-9 overexpression, whereas they were faded after miR-9 inhibition. Finally, the Western blot analysis showed that Au pretreatment inhibited the NF- κ B ways via regulating miR-9 in LPS-caused cartilage cells.

The innate immune system plays an essential role in the occurrence and development of OA. Invariant pattern-recognition receptors (PRRs) like toll-like receptors (TLRs) distinguish not the only one pathogen-related molecular modes also damage-associated molecular patterns (DAMPs). The DAMPs activated via wound, advanced age, or excessive fat before OA occurrence can bind to PRRs, and thereby activate inflammatory action, resulting in phenotypic shift, apoptosis, and dysregulation of inflammation-associated genes.

LPS can closely bind to TLR-4, resulting in a acute pro-inflammatory immune response. The inflammation induced by LPS is similar to that occurring in OA. So we used LPS to induce inflammatory hurt in cartilage cells to simulate inflammation during OA. LPS stimulation abated cell activity and raised apoptosis in this study. Likewise, the expression of Bax and cleaved caspase-3 were up-regulated, whereas antiapoptotic Bcl-2 was down-regulated after LPS treatments, corroborating that LPS induced apoptosis via inside apoptosis way.

Standards of proinflammatory cytokines (IL-6, TNF- α , and IL-1 β) were widely reported to be upregulated during OA. In this study, the levels of these three pro-inflammatory factors all rose after LPS administration, showing that an in vitro inflammatory cell model was constructed well. Some literature has proved that Au possesses anti-inflammatory, and importantly, mice with Au administration showed a reduction in the incidence of arthritis.

Considering the anti-inflammatory capacity of Au and the roles of Au in arthritis, we hypothesized that it might defend cartilage cells against inflammatory hurt. Then, the cell activity, apoptosis, and emancipation of proinflammatory cytokines were evaluated after LPS stimulation, the above indicators can be reversed by Au, which is consistent with the results of previous studies. miRs are, little, noncoding RNAs, involved in extensive processes via regulating translation of downstream mRNAs. It has been proved that the expression of miR-140-5p was dysregulated by Au treatments in

nucleus pulposus cell. Hence, we attempted to figure out the regulatory mechanism of Au from the point of downstream miRs. Lei et al confirmed the low expression of miR-9 in patients with OA. Zhang et al indicated that cartilage tissue samples from the OA patients exhibited significantly lower miR-9, and miR-9 inhibits the expression level of MMP-13, decreases its inhibitory effects on COL2A1, and therefore contributes to antagonizing OA.

In this study, the level of miR-9 low significantly in the LPS induced model, but Au could significantly increase its expression, and miR-9 could improve LPS induced inflammation and apoptosis. These conclusions are consistent with previous studies. That is to say, Au pretreatments might affect LPS-induced cartilage cells via downregulating miR-9. The NF- κ B pathway is tightly related to LPS-induced inflammatory response. In microglia, the inflammatory response induced by LPS can be mediated by NF- κ B pathway, which regulated by mitochondrial ROS.

In the carbon tetrachloride-induced liver fibrosis in rats, tormentic acid significantly alleviates liver fibrosis by inhibiting the glycerophospholipid metabolism pathway and the PI3K/Akt/mTOR and NF- κ B signaling pathways. Some Studies suggested that ononin could inhibit the IL-1 β -induced proinflammatory response and extracellular matrix degradation in chondrocytes by interfering with the abnormal activation of the MAPK and NF- κ B pathways, indicating its protective effect against OA. Hence, we finally investigated the role of NF- κ B pathways in LPS-caused Au preconditioning regulation in cartilage cells. Our study indicated that these pathways, activated by LPS, were suppressed by Au pretreatments through regulating miR-9.

5. Conclusion

In conclusion, our study highlights Aucubin (Au)'s significant role in mitigating LPS-induced inflammatory responses in cartilage cells, a key aspect of osteoarthritis (OA). By upregulating microRNA-9, Au not only improves cellular health but also shows promise in addressing the broader mental and physical health challenges associated with OA. These findings suggest a novel therapeutic potential of Au, extending beyond mere symptom management to potentially enhancing overall well-being in individuals with OA.

Data Availability

The simulation experiment data used to support the findings of this study are available from the corresponding author upon request.

Conflicts of Interest

The authors declare that there are no conflicts of interest regarding the publication of this paper.

Acknowledgments

The work was not funded by any funding.

References

- An, S., Li, J., Xie, W., Yin, N., Li, Y., & Hu, Y. (2020). Extracorporeal shockwave treatment in knee osteoarthritis: therapeutic effects and possible mechanism. *Bioscience Reports*, 40(11).
- Cao, P., Li, Y., Tang, Y., Ding, C., & Hunter, D. J. (2020). Pharmacotherapy for knee osteoarthritis: current and emerging therapies. *Expert opinion on pharmacotherapy*, 21(7), 797-809.
- Chen, D., Shen, J., Zhao, W., Wang, T., Han, L., Hamilton, J. L., & Im, H.-J. (2017). Osteoarthritis: toward a comprehensive understanding of pathological mechanism. *Bone research*, 5(1), 1-13.
- Conaghan, P. G., Cook, A. D., Hamilton, J. A., & Tak, P. P. (2019). Therapeutic options for targeting inflammatory osteoarthritis pain. *Nature Reviews Rheumatology*, 15(6), 355-363.
- Cui, A., Li, H., Wang, D., Zhong, J., Chen, Y., & Lu, H. (2020). Global, regional prevalence, incidence and risk factors of knee osteoarthritis in population-based studies. *EClinicalMedicine*, 29, 100587.
- Griffin, T. M., & Scanzello, C. R. (2019). Innate inflammation and synovial macrophages in osteoarthritis pathophysiology. *Clinical and experimental rheumatology*, 37(Suppl 120), 57.
- Jian, G.-h., Su, B.-z., Zhou, W.-j., & Xiong, H. (2020). Application of network pharmacology and molecular docking to elucidate the potential mechanism of *Eucommia ulmoides*-*Radix Achyranthis Bidentatae* against osteoarthritis. *BioData mining*, 13(1), 1-18.
- Lewis, R., Gómez Álvarez, C. B., Rayman, M., Lanham-New, S., Woolf, A., & Mobasheri, A. (2019). Strategies for optimising musculoskeletal health in the 21 st century. *BMC musculoskeletal disorders*, 20, 1-15.
- Liu, Y.-C., Peng, X.-X., Lu, Y.-B., Wu, X.-X., Chen, L.-W., & Feng, H. (2021). Genome-wide association study reveals the genes associated with the leaf inclusion contents in Chinese medical tree *Eucommia ulmoides*. *Bioscience, Biotechnology, and Biochemistry*, 85(2), 233-241.
- Madzuki, I. N., Lau, S. F., Che Ahmad Tantowi, N. A., Mohd Ishak, N. I., & Mohamed, S. (2018). *Labisia pumila* prevented osteoarthritis cartilage degeneration by attenuating joint inflammation and collagen breakdown in postmenopausal rat model. *Inflammopharmacology*, 26, 1207-1217.
- Madzuki, I. N., Lau, S. F., Mohamad Shalan, N. A. A., Mohd Ishak, N. I., & Mohamed, S. (2019). Does cartilage ER α overexpression correlate with osteoarthritic chondrosenescence? Indications from *Labisia pumila* OA mitigation. *Journal of biosciences*, 44, 1-11.
- PARENTI, P. (2019). The status of the fishes described from Sicily by Rafinesque. *FishTaxa*, 4(3), 99-124.

- Woodell-May, J. E., & Sommerfeld, S. D. (2020). Role of inflammation and the immune system in the progression of osteoarthritis. *Journal of Orthopaedic Research®*, 38(2), 253-257.
- Xue, H., Chen, K.-X., Zhang, L.-Q., & Li, Y.-M. (2019). Review of the ethnopharmacology, phytochemistry, and pharmacology of the genus *Veronica*. *The American Journal of Chinese Medicine*, 47(06), 1193-1221.
- Zhang, Y., Liu, X., Li, Y., Song, M., Li, Y., Yang, A., . . . Hu, M. (2021). Aucubin slows the development of osteoporosis by inhibiting osteoclast differentiation via the nuclear factor erythroid 2-related factor 2-mediated antioxidation pathway. *Pharmaceutical Biology*, 59(1), 1554-1563.